

KINETICS OF THERMAL DECOMPOSITION OF NICKEL SULFATE HEXAHYDRATE

J. Straszko, J. Mozejko and M. Olszak-Humienik

Department of Engineering and Physical Chemistry, Technical University of Szczecin, Szczecin, Poland

Abstract

The paper describes the kinetics of all the recorded steps of thermal decomposition of nickel sulfate hexahydrate in air.

The thermal decomposition of the salt in air led to NiO at about 1060 K. The kinetic parameters, the activation energy E and the preexponential factor A , and the thermodynamic parameters, the entropy, enthalpy and free energy of activation were evaluated for the dehydration and decomposition reactions. Tentative reaction mechanisms are suggested for each step of the thermal decomposition.

Keywords: kinetics of thermal decomposition, thermal decomposition

Introduction

The thermal decomposition of nickel sulfate has been investigated as part of a research programme on the thermal dissociation of sulfates of elements in the fourth period of Mendeleev's classification. Besides the academic interest, these elements have always played an important role in metallurgy.

A number of papers have reported on the pyrolysis of nickel sulfate [1-6], but one important problem is the explanation of the inconsistencies in the kinetic parameters obtained by different authors. The published data are incompatible as regards particular steps of decomposition. The intermediate hydrates differ in composition, depending on the heating rate and the starting hydrates. All authors have reported NiO as the end-product of the thermal decomposition.

The aims of the present investigation were to study the nonisothermal decomposition of $\text{NiSO}_4 \cdot 6\text{H}_2\text{O}$ in air, to characterize the intermediates and to calculate the kinetic parameters for particular stages of the dissociation.

The data relating to the TG curves were used to derive the mechanism of the individual stages, and their kinetic and thermodynamic parameters were calculated.

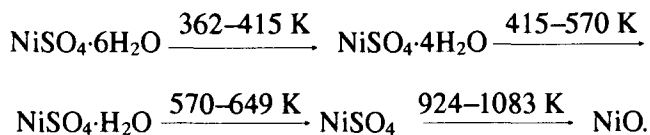
Experimental

The starting material, $\text{NiSO}_4 \cdot 6\text{H}_2\text{O}$, was produced by P. P. H. Polskie Od-czynniki Chemiczne, Gliwice.

The thermogravimetric measurements were carried out on a Hungarian MOM 1500 derivatograph. The operational characteristics were as follows: heating rate: $5 \text{ deg} \cdot \text{min}^{-1}$, sample size: 700 mg, atmosphere: static air, tempera-ture range: 20–1000 °C.

Results and discussion

Figure 1 illustrates the non-isothermal decomposition of one sample of $\text{NiSO}_4 \cdot 6\text{H}_2\text{O}$. Our results suggest the following reactions in air:



The TG curve indicated that the water loss started from 362 K. This curve suggested the loss of two molecules of water. This corresponded to the mass loss data (found 13.4%, calc. 13.7%) observed the TG curves.

The DTA curves recorded in air showed a first sharp endothermic peak at about 391 K.

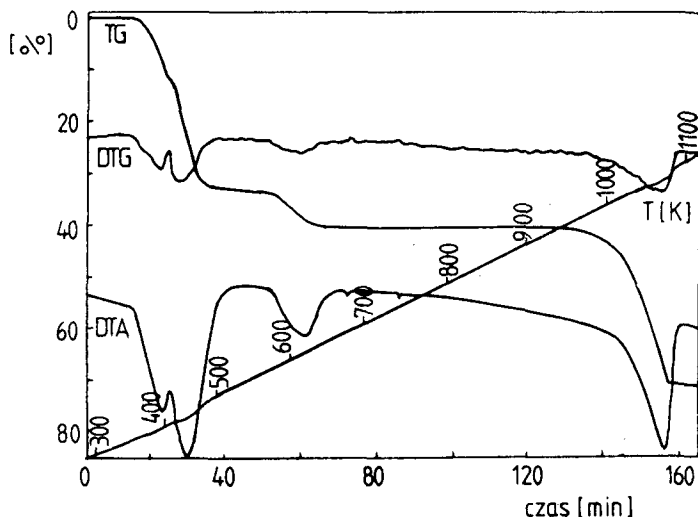


Fig. 1 Thermal decomposition of $\text{NiSO}_4 \cdot 6\text{H}_2\text{O}$

The endothermic peak at around 420 K in the DTA curve and the slope in the TG curve up to 415 and 570 K, with a mass loss of 19.9%, might be due to the simultaneous evolution of three molecules of water.

The mass losses beginning at 570 K in the TG curves corresponded to formation of the anhydrous compound.

The endothermic peak connected with removal of the last water had its minimum at about 613 K, with a mass loss of 6.6%.

The step section of the TG curve ended at 1083 K with a mass loss of 29.7% which might indicate formation of the stable compound NiO (calc. mass loss 30.5%). The DTA peak at around 1060 K, with a strong endoeffect, corresponded to this overall decomposition step.

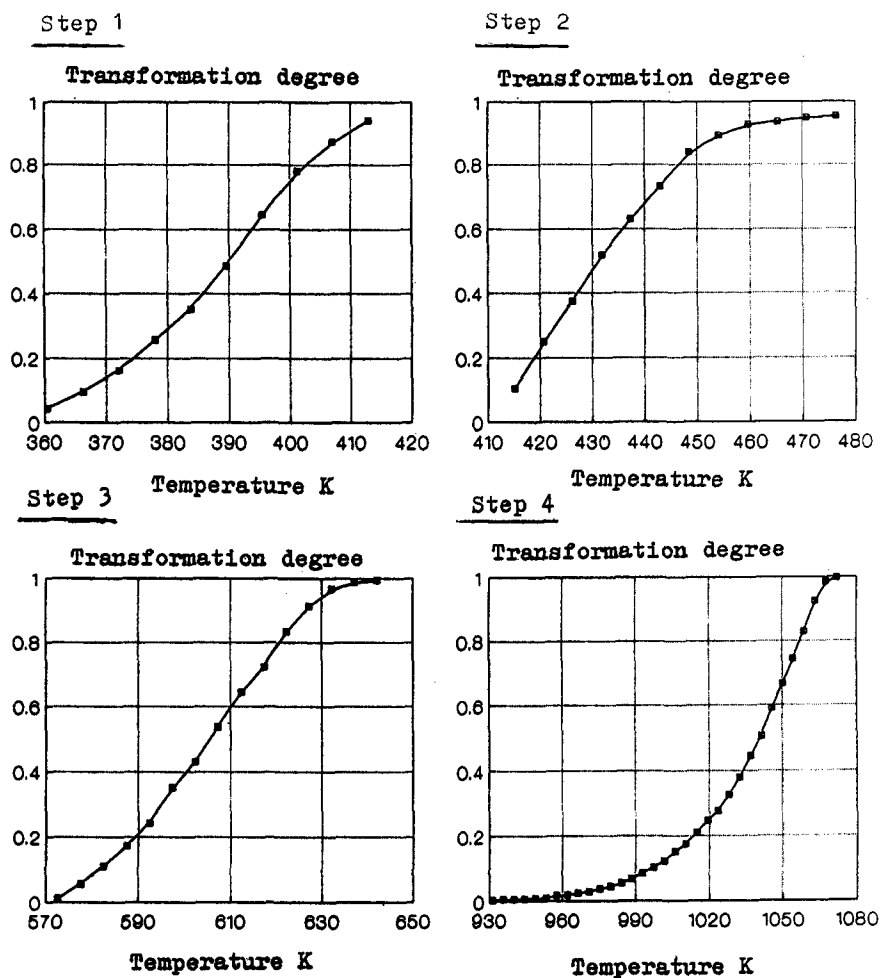


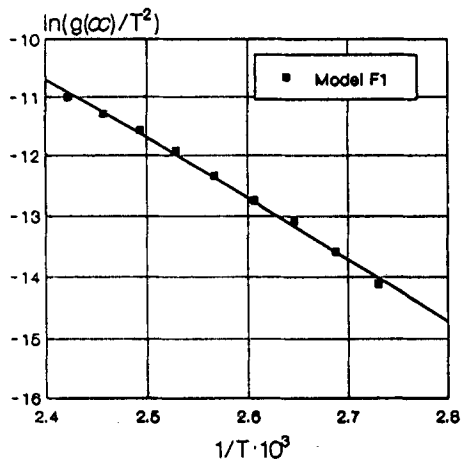
Fig. 2 α vs. T relations for particular steps of decomposition of $\text{NiSO}_4 \cdot 6\text{H}_2\text{O}$

From the mass loss observed in the TG curves, the α vs. T relations were estimated. These dependences for all the stages of the decomposition are depicted in Fig. 2.

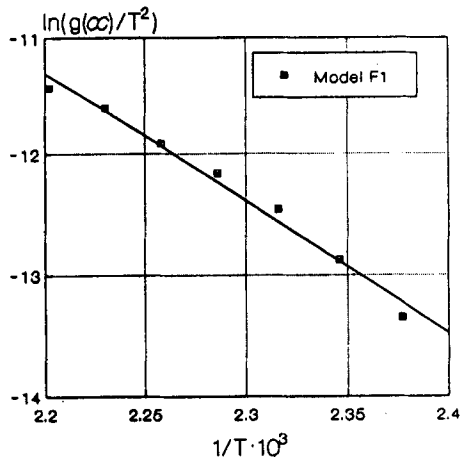
These dependences were processed by a special computer program based on a least-squares procedure.

From the $\alpha(T)$ dependence and well-known kinetic models [1], the $g(\alpha)$ functions which best described the experimental results on the decomposition were chosen.

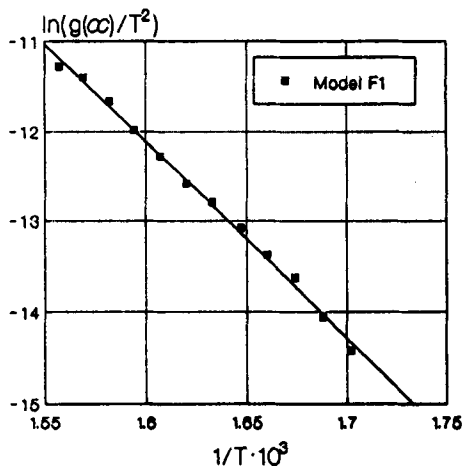
Step 1



Step 2



Step 3



Step 4

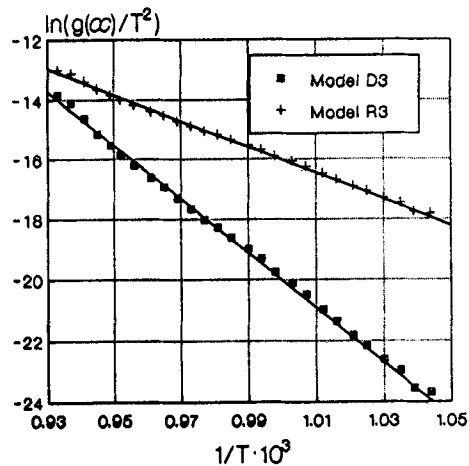


Fig. 3 $\ln(g(\alpha)/T^2)$ vs. $1/T$ relations for the best-fitting models

Table 1 Results of kinetic calculations

Stage	$g(\alpha)$	$E /$ $\text{kJ}\cdot\text{mol}^{-1}$	$A /$ min^{-1}	r	F	s	$\Delta S^\ddagger /$ $\text{J}\cdot(\text{mol}\cdot\text{K})^{-1}$	$\Delta H^\ddagger /$ $\text{kJ}\cdot\text{mol}^{-1}$	$\Delta G^\ddagger /$ $\text{kJ}\cdot\text{mol}^{-1}$	
1	D1	117.71	5.97E+14	0.9753	137	0.362	-6.7	114.5	117.1	
	D2	132.31	3.89E+16	0.9847	223	0.318	28.1	129.1	118.1	
	D3	151.90	8.51E+18	0.9935	537	0.235	72.9	148.6	120.1	
	D4	138.71	1.08E+17	0.9882	292	0.291	36.6	135.5	121.1	
	F1	83.54	4.29E+10	0.9981	1823	0.070	-86.0	80.3	113.9	
	A2	38.54	2.53E+04	0.9977	1494	0.036	-205.3	35.3	115.6	
	A3	23.54	1.86E+02	0.9971	1208	0.024	-246.1	20.3	116.6	
	R1	55.63	3.45E+06	0.9723	121	0.182	-164.4	52.4	116.7	
	R2	67.90	2.23E+08	0.9889	310	0.138	-129.7	64.6	115.4	
	R3	72.72	1.13E+09	0.9929	486	0.118	-116.2	69.5	114.9	
	2	D1	112.19	3.31E+12	0.9641	66	0.256	-50.4	108.7	129.9
		D2	131.88	5.78E+14	0.9755	98	0.246	-7.5	128.4	131.5
		D3	158.22	4.53E+17	0.9864	180	0.218	47.9	154.7	134.6
D4		140.50	2.46E+15	0.9798	120	0.238	4.5	137.0	135.1	
F1		89.94	1.74E+10	0.9925	330	0.092	-94.1	86.4	125.9	
A2		41.34	1.44E+04	0.9910	275	0.046	-210.5	37.8	126.2	
A3		25.14	1.19E+02	0.9891	225	0.031	-250.4	21.6	126.7	
R1		52.46	2.19E+05	0.9590	57	0.128	-187.9	49.0	127.8	
R2		69.01	3.32E+07	0.9800	121	0.116	-146.1	65.5	126.8	
R3		75.48	2.32E+08	0.9850	163	0.109	-130.0	72.0	126.5	
3	D1	234.27	1.13E+19	0.9636	117	0.360	71.5	229.2	185.4	
	D2	269.83	9.62E+21	0.9761	181	0.333	127.6	264.7	186.6	
	D3	319.39	9.54E+25	0.9886	389	0.269	204.1	314.3	189.3	
	D4	285.94	9.15E+22	0.9810	230	0.313	146.3	280.8	191.2	
	F1	182.44	1.09E+15	0.9956	1011	0.095	-5.4	177.3	180.6	
	A2	86.16	3.40E+06	0.9950	891	0.048	-168.2	81.1	184.1	
	A3	54.06	4.25E+03	0.9943	780	0.032	-223.8	49.0	186.0	
	R1	112.08	3.88E+08	0.9603	107	0.180	-128.8	107.0	185.9	
	R2	142.45	2.45E+11	0.9823	248	0.151	-75.2	137.4	183.4	
	R3	154.64	3.19E+12	0.9878	363	0.135	-53.9	149.5	182.5	
4	D1	677.65	8.66E+32	0.9962	3794	0.289	332.8	668.8	316.3	
	D2	706.34	1.61E+34	0.9982	8136	0.206	357.0	697.5	319.3	
	D3	743.47	5.68E+35	0.9992	17492	0.148	386.7	734.7	325.0	
	D4	718.42	2.44E+34	0.9988	11836	0.174	360.5	709.6	327.6	

Table 1 Continued

Stage	$g(\alpha)$	$E /$ $\text{kJ}\cdot\text{mol}^{-1}$	$A /$ min^{-1}	r	F	s	$\Delta S^* /$ $\text{J}\cdot(\text{mol}\cdot\text{K})^{-1}$	$\Delta H^* /$ $\text{kJ}\cdot\text{mol}^{-1}$	$\Delta G^* /$ $\text{kJ}\cdot\text{mol}^{-1}$
4	F1	384.02	2.94E+18	0.9976	5977	0.131	55.7	375.2	316.2
	A2	183.70	1.47E+08	0.9974	5520	0.065	-141.5	174.9	324.8
	A3	116.93	4.60E+04	0.9972	5077	0.043	-208.6	108.1	329.1
	R1	330.52	3.29E+15	0.9960	3579	0.145	-0.7	321.7	322.5
	R2	354.25	6.74E+16	0.9989	13409	0.080	24.4	345.4	319.6
	R3	363.43	2.16E+17	0.9991	16625	0.074	34.0	354.6	318.6

The correlation coefficient (r), the standard deviation (s) and Snedecor's variable (F) were calculated to aid selection of the $g(\alpha)$ function.

Figure 3 presents the dependences $\ln[g(\alpha)/T^2]$ vs. $1/T$ for the best-fitting models of decomposition.

Kinetic and thermodynamic parameters were calculated from the Arrhenius and Eyring equations by means of the Coats-Redfern method for the separate steps. These parameters are listed in Table 1.

It was found that all stages of the dehydration process are regulated by the random nucleation model F1 $\{g(\alpha) = -\ln(1-\alpha)\}$.

The decomposition of anhydrous nickel sulfate is controlled by the three-dimensional diffusion model D3 $\{g(\alpha) = 3/2[1-(1-\alpha)^{1/3}]^2\}$ or the contracting volume model R3 $\{g(\alpha) = 3[1-(1-\alpha)^{1/3}]\}$. These models of decomposition of NiSO_4 are possible because the edge dimensions of the crystal are close ($a = 6.338$, $b = 7.842$ and $c = 5.155$) and the reaction occurs equally at all faces of a cube. Our results for this stage of decomposition are different from those presented for a constant rate of dissociation [1], where $\Delta E = 269 \text{ kJ}\cdot\text{mol}^{-1}$ and $\Delta H = 236 \text{ kJ}\cdot\text{mol}^{-1}$.

The changes in reaction rate for particular steps of decomposition of $\text{NiSO}_4\cdot 6\text{H}_2\text{O}$ as a function of temperature are presented in Fig. 4.

It can be seen that the lowest maximum reaction rate is that for decomposition of anhydrous nickel sulfate.

Conclusions

The results presented above show that the particular stages of thermal dehydration of nickel sulfate hexahydrate in air atmosphere are governed by the random nucleation model (F1).

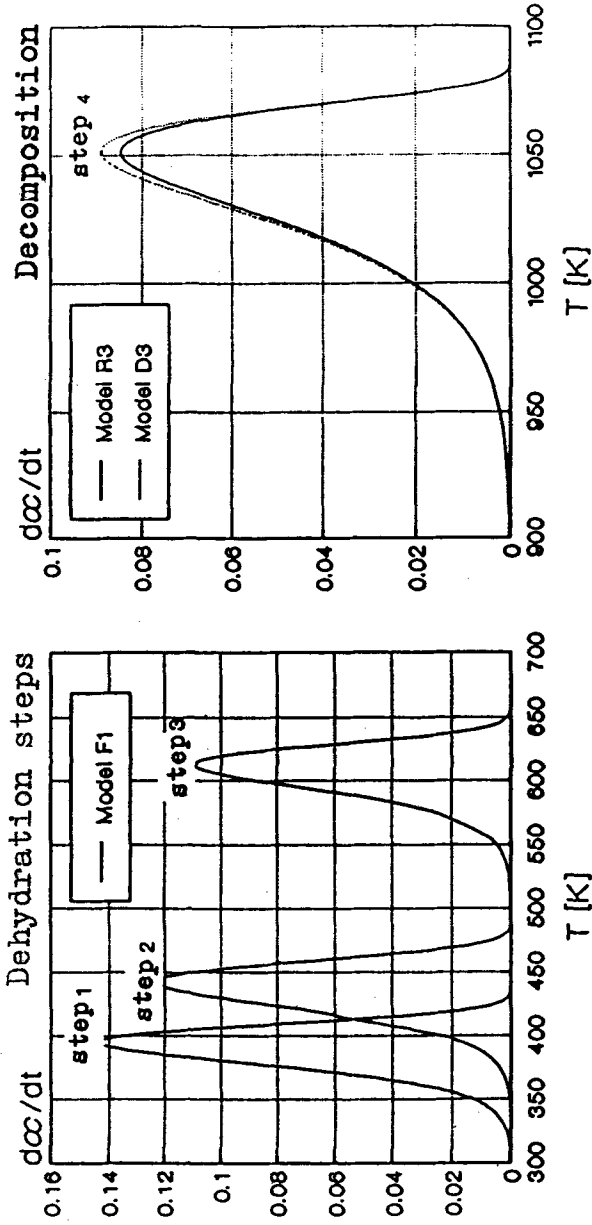


Fig. 4 Dependences of reaction rate $d\alpha/dt$ on temperature for particular steps of decomposition of $\text{NiSO}_4 \cdot 6\text{H}_2\text{O}$

The experimental results on the decomposition of anhydrous nickel sulfate confirm that it is impossible to choose one kinetic model from dynamic measurements. This step of decomposition is regulated by model D₃ or R₃.

References

- 1 Chemical kinetics, Vol. 22, p. 121, 178, Elsevier Scientific Publishing Company, Amsterdam, Oxford, New York, 1980.
- 2 D. Shultze, Termiczna analiza różnicowa, PWN, Warszawa 1974.
- 3 Atlas of thermoanalytical curves (Vol. 5), Akadémiai Kiadó, Budapest 1976.
- 4 G. G. T. Guarini and M. Rustici, *J. Thermal Anal.*, 34 (1988) 487.
- 5 M. Maneva, D. Rizowa, L. Genov and G. Liptony, *J. Thermal Anal.*, 36 (1990) 915.
- 6 L. G. Berg and V. P. Korirzina, *Zh. Neorg. Khim.*, 9 (1964) 29.

Zusammenfassung — Vorliegend werden alle aufgezeichneten Schritte der thermischen Zersetzung von Nickelsulfathexahydrat in Luft beschrieben.

Die thermische Zersetzung des Salzes führt zu NiO in Luft bei etwa 1060 K. Die kinetischen Parameter, d.h. die Aktivierungsenergien E und die präexponentiellen Koeffizienten A sowie die thermodynamischen Parameter Entropie, Enthalpie und freie Energie der Aktivierung von Dehydratations- und Zersetzungsreaktionen wurden geschätzt. Für jeden Schritt der thermischen Zersetzung wurde ein vorläufiger Reaktionsmechanismus vorgeschlagen.